Monthly Notices of the ROYAL ASTRONOMICAL SOCIETY

MNRAS **467,** 2966–2979 (2017) doi:10.1093/mnras/stx145

Sky Quality Meter measurements in a colour-changing world

A. Sánchez de Miguel,[1,2,3★†] M. Aubé,[1★†] J. Zamorano,[2] M. Kocifaj,[4,5] J. Roby[1] and C. Tapia[2]

[1]*Cégep de Sherbrooke, 475 rue du Cégep, Sherbrooke, J1E 4K1, Canada*
[2]*Dep. Astrofísica y CC. de la Atmósfera, CC. Fisicas, Avd Complutense s/n, E-28040 Madrid, Spain*
[3]*Instituto de Astrofísica de Andalucía-CSIC, Glorieta de la Astronomía s/n, E-18008 Granada, Spain*
[4]*ICA, Slovak Academy of Sciences, Dúbravská Road 9, 84503 Bratislava, Slovakia*
[5]*Faculty of Mathematics, Physics, and Informatics, Comenius University, Mlynská dolina, 84248 Bratislava, Slovakia*

Accepted 2017 January 17. Received 2017 January 12; in original form 2016 April 15

ABSTRACT

The Sky Quality Meter (SQM) has become the most common device used to track the evolution of the brightness of the sky from polluted regions to first-class astronomical observatories. A vast database of SQM measurements already exists for many places in the world. Unfortunately, the SQM operates over a wide spectral band and its spectral response interacts with the sky's spectrum in a complex manner. This is why the optical signals are difficult to interpret when the data are recorded in regions with different sources of artificial light. The brightness of the night sky is linked in a complex way to ground-based light emissions, while taking into account atmospheric-induced optical distortion as well as spectral transformation from the underlying ground surfaces. While the spectral modulation of the sky's radiance has been recognized, it still remains poorly characterized and quantified. The impact of the SQM's spectral characteristics on sky-brightness measurements is analysed here for different light sources, including low- and high-pressure sodium lamps, PC-amber and white LEDs, metal halide and mercury lamps. We show that a routine conversion of radiance to magnitude is difficult, or rather impossible, because the average wavelength depends on actual atmospheric and environment conditions, the spectrum of the source and device-specific properties. We correlate SQM readings with both the Johnson astronomical photometry bands and the human system of visual perception, assuming different lighting technologies. These findings have direct implications for the processing of SQM data and for their improvement and/or remediation.

Key words: atmospheric effects – instrumentation: miscellaneous – instrumentation: photometers – light pollution – methods: data analysis – techniques: spectroscopic.

1 INTRODUCTION

The Sky Quality Meter (SQM) has been widely used in studies related to light pollution (Falchi 2011; Kyba et al. 2012, 2015; Pun & So 2012; Puschnig, Posch & Uttenthaler 2014). Most research has been done over a period of time characterized by a very slow change in illumination technologies and their spectra. With the massive arrival of light-emitting diodes (LED) in street lighting, the situation is changing very rapidly. We can expect an exponential growth in the replacement of incandescent lamps by LED lamps, as happened in the 1970s (Riegel 1973). This projection is confirmed by the International Space Station (ISS) observations (Sanchez de Miguel 2015b) and the market projections for indoor illumination (Danish Energy Agency, Energy Piano & CLASP European Programme 2015; Katona, Pattison & Paolini 2016). The change in the colour of the sky during the night was detected for the first time by Kyba et al. (2012). The authors used SQMs with special filters to monitor the change of colour. At that time, no link between the colour of the sky and the change in lamp spectra had been established. Sánchez de Miguel (2015a) outlined a change in the spectra of the sky based on analysis with an all-sky CCD camera with Johnson's filters. To monitor this change correctly, we must have detectors with minimal spectral capabilities, like radiometers with colour filters, colour cameras or even spectrometers. However, such instrumentation is relatively expensive and thus cannot easily be spread all over the world. On the other hand, the SQM is very cheap and easy to use, making it a nice instrument for creating global

★ These authors contributed equally to this work.
† E-mail: asanchez@iaa.es (ASM); martin.aube@cegepsherbrooke.qc.ca (MA)

measuring networks. This type of instrument is useful to track temporal and geographical variations in sky brightness (SB), but without any colour information. In this article, we want to outline how the broad-band spectral response of the SQM reacts to variations in the spectrum of the source for a variety of lighting technologies and for the combination of some other sources of natural origin (e.g. scattered moonlight, background stars, natural airglow).

In the short-term, the spectrum of the zenith sky changes slightly with changes in atmospheric aerosol content, but more importantly because of clouds. The extinction of ornamental lights and office windows, car headlights (traffic), the phase of the moon and the angle of its altitude in the sky also play an important role. The coordinates of the zenith in the Galactic coordinate system and the geographical latitude of solar activity also affect the spectrum of the sky. Generally, the spectra of street lights do not change significantly in the short-term, but on a longer time-scale street lamp conversion/replacement can also modify the spectrum of the sky significantly. Currently, the world is experiencing a massive transition in lighting technology, in which entire cities can change from classical high-intensity discharge (HID) lamps (e.g. high-pressure sodium or HPS) to white LEDs. Under such important natural and human-made changes, how can we prove that the temporal variations in SB as detected by a broad-band instrument like the SQM are representative of the variations in SB that should be detected by the human eye? Moreover, how can we analyse the human-made variation of the SB, excluding the natural variations of the SB? In order to provide basic quantitative tools to improve the tracking of human-made or artificial SB, we will analyse the impact of each variable component on the reading of the SQM by simulating the detected signal of the SQM. To accomplish this simulation, we multiply the different source spectra by the spectral response of the SQM-L. Using many analyses, we infer the relationship between SQM readings with human-eye sensitivity under the scotopic and photopic regimes for different lighting technologies and we compare the relationship of the SQM readings with the Johnson *V* astronomical photometry band.

2 THE CHARACTERISTICS OF THE SQM

The SQM is a simple and portable device intended to facilitate the measurement of SB by non-highly qualified personnel. Up to now, there have been two generations of this device and soon a new one will be released. The system is composed of a silicon photodiode as detector (ams-TAOS TSL237S), partly covered by a near-infrared rejection filter. The spectral response of the device tries to mimic that of the human eye under the photopic regime. The device also has a light-to-frequency converter with a significant response up to the near-infrared. The spectral sensitivity of the photodiode, combined with the transmission of the HOYA CM-500 near-infrared cut-off filter, provides a final spectral response overlapping the Johnson *B* and *V* bands used in astronomical photometry (wavelength range 320–720 nm: Johnson & Morgan 1953). Although it is very user-friendly (aim the photometer to the zenith, push the button and read the data on the display), it is nevertheless accurate enough to perform scientific research (Cinzano 2005). The SQM photometers have a quoted systematic uncertainty of 10 per cent (0.1 mag arcsec^{-2}). Its use has become very popular among researchers and amateur astronomers, along with interested members of associations that fight against light pollution.

The SQM-L model, the simplest one, is a hand-held photometer intended for gathering data in the field. When used with a photographic tripod, one can measure at different angles and build a map

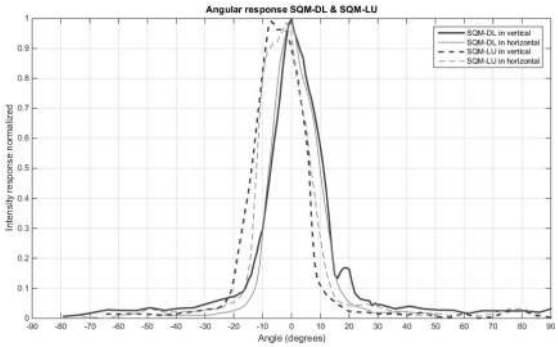

Figure 1. SQM angular response from two SQMs in magnitude scale.

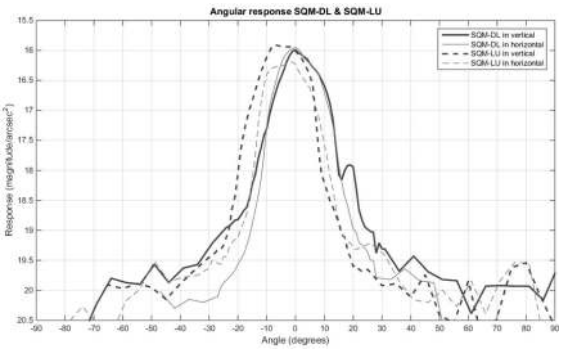

Figure 2. SQM angular response from two SQMs in intensity scale.

of the all-sky brightness (Zamorano et al. 2013). For mapping a geographical area, one can move to selected locations of a grid, taking the measurements one by one (Biggs et al. 2012; Falchi et al. 2016; Zamorano et al. 2016). The SQM-LU and SQM-LE units should be linked to a computer by means of USB or ethernet connection, respectively. These models are designed to be used at a fixed monitoring station to take and register data continually. These connected devices could also be used to map extended areas using a vehicle and GPS information.

All the models described above share the same characteristics. The full width at half-maximum (FWHM) of the angular sensitivity is $\sim$20° (Cinzano 2007). The sensitivity to a point source $\sim$19° off-axis is a factor of 10 lower than that on-axis. A point source 20° and 40° off-axis would register 3.0 and 5.0 astronomical magnitudes fainter, respectively (Unihedron SQM-L manual).

We found a high variability in the shape of the angular response of the SQM. However, the FWHM remains constant at around $\sim$20° (see Figs 1 and 2).

The source of this variability comes from inproper alignment of the optics of the SQM (den Outer et al. 2011, 2015; Bará et al. 2015).

The AB magnitudes for any photometric band are determined by equation (1) (Fukugita, Shimasaku & Ichikawa 1995):

$$m_{\rm AB} = -2.5\ \log_{10} \frac{\int_0^\infty T(\lambda)\,\phi(\lambda)\,{\rm d}\lambda}{\int_0^\infty T(\lambda)\,\phi_{\rm AB}(\lambda)\,{\rm d}\lambda}, \qquad (1)$$

where $T(\lambda)$ is the spectral sensitivity of the observation band, $\phi(\lambda)$ is the spectrum of the source and $\phi_{\rm AB}(\lambda)$ is the reference spectrum, defined for a source of constant spectral density flux of 3631 Jy over the entire spectral range of the band.

The conversion from AB magnitudes (Oke & Gunn 1983), an astronomical magnitude system, to radiance (R) can be done using the following relationship (this work):

$$m_{\rm AB} = -2.5\ \log(R) - 5\log\bar{\lambda} - 2.41, \quad (2)$$

where R is expressed in erg s^{-1} cm^{-2} Å^{-1} and $\bar{\lambda}$ is the average wavelength of the band. The average wavelength is defined by the following equation:

$$\bar{\lambda} = \frac{\int_0^\infty T(\lambda)\lambda\,{\rm d}\lambda}{\int_0^\infty T(\lambda)\,{\rm d}\lambda}, \quad (3)$$

where $T(\lambda)$ is the spectral sensitivity of the observation band (including the detector response).

Using equations (1) and (2), we can create synthetic photometry measurements from any spectral source and any spectral band.

The SQM calibration is made using the manufacturer reference lamp.[1] To convert SQM magnitudes to astronomical V Johnson magnitudes, we need to apply a shift of 0.35 mag (Cinzano 2005). However, Cinzano (2005) has used the Vega magnitudes, which produces problems for converting into SI units, so we will use the AB magnitude system, which does not have that problem. We thus only need to use the transformation $(SQM - V)_{\rm AB} = (SQM - V)_{\rm Vega} - 0.04$, based on equation (3). Hence, the SQM offset between the $(SQM_{\rm O} - V)_{\rm Vega} = (SQM - V)_{\rm Vega} - 0.35 = (SQM - V)_{\rm AB} - 0.31$, where $SQM_{\rm O}$ represents mag$_{SQM}$ from the readings of the SQM devices. This should be considered as a first-order correction, because a correct relationship needs to take into consideration the spectra of the source. In this article, we will write $SQM_{\rm AB}$ to express the SQM reading using the AB magnitude definition and $SQM_{\rm O}$ to express the SQM readings with the instrument factory calibration as performed by Unihedron. Knowing this, we can convert easily from $SQM_{\rm O}$ to radiance units with equation (2) by

$$SQM_{\rm O} + 0.31 = SQM_{\rm AB} = -2.5\ \log(R) - 5\log\overline{5418\,\text{Å}} - 2.41. \quad (4)$$

From this equation is possible to obtain, through basic operations,

$$R' = 0.0270\,038 \times 10^{-0.4\ SQM_{\rm O}}, \quad (5)$$

where R is in units of erg s^{-1} cm^{-2} Å^{-1} arcsec^{-2}, R' is in units of W cm^{-2} sr^{-1}, $SQM_{\rm O}$ is in units of mag$_{SQM}$ arcsec^{-2} and 5418 Å is the effective wavelength of the SQM band.

We have combined the spectral tranfer functions of the optical parts of the SQM photometers to build the theoretical or expected response of the device. Instead of using the manufacturer's information, we have measured the spectral response of the detector and the transmission curve of the filter. The window, infrared rejection filter (Hoya 500) and lens assembly of one SQM photometer were removed to determine the spectral response of the TSL237 detector itself (see Fig. 3). The light beam from a monochromator was fed to an integrating sphere, with the SQM detector observing through one other port of the sphere.

The measured SQM total response should be the same as the spectral response that we have determined by combining the measured responses for each optical component. Our experiment shows that important differences arise in the form of a prominent infrared tail (see Figs 3 and 4) in the total SQM response. We had similar results for three SQM units that we had in hand (SQM-LU, SQM-LE and SQM-DL). This unexpected near-infrared response is caused by the fact that the infrared rejection filter does not cover the optical path fully. The Hoya 500 filter can be recognized as a square blue glass located behind the lens assembly. Also, there is a lack of sensitivity in the UV part, probably because of the transmittance of the lens used.

[1] Anthony Tekatch, Unihedron, personal communication.

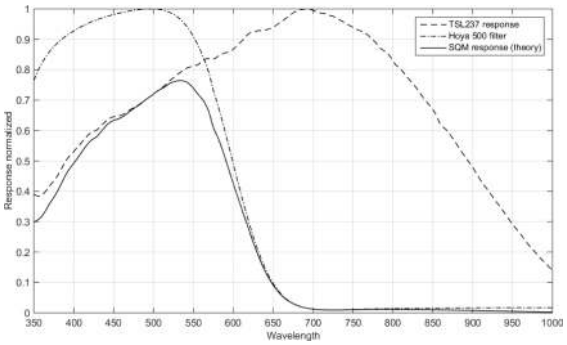

Figure 3. Spectral response of some optics components of the SQM.

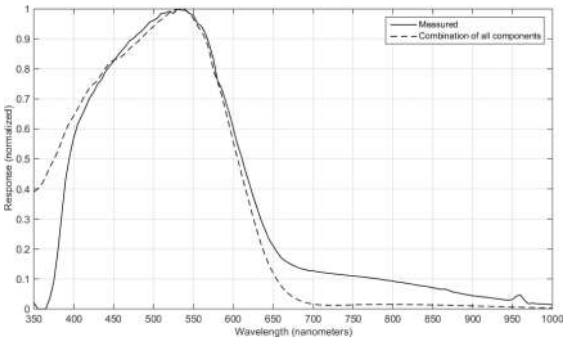

Figure 4. SQM spectral response. The dashed line corresponds to the combination of all the spectral response/transmission values of the components, while the black line is the total measured response.

2.1 SQM readings versus photopic, scotopic vision and Johnson photometric systems

Ever since Johnson & Morgan (1953) defined the first astronomical photometric system, the sky brightness has been measured by astronomers. Magnitudes in the AB system can be converted to other systems. However, because all magnitude systems involve integration of some assumed source spectrum over some assumed spectral range or band, such conversions are not necessarily trivial to determine. Various authors have computed conversions for standard situations. Johnson & Morgan (1953) clearly explained that, even if the colour of the V_j filter is yellow, it does not mean that the V_j is representative of the human vision response. In fact, the V_j band peaks at the central point of daylight human vision but the bandwidth is not broad enough to represent all contributions to human vision. The accepted daylight human light curve, dominated by the cones, was set by CIE 1931 (Smith & Guild 1931) as the $V(\lambda)$ curve, also known as photopic vision. Low light level vision, dominated by the rods, has a different response and is called scotopic vision (Judd 1951). Now the CIE has recently approved an intermediate vision regime based on Rea et al. (2004) and Eloholma & Halonen (2006), the so-called 'mesopic vision'. Mesopic vision involves both cones and rods, with various proportions depending on the light level.

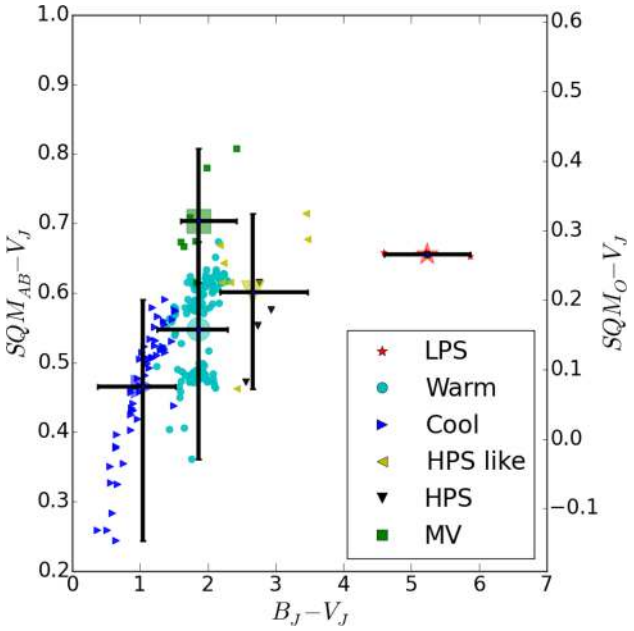

Figure 5. Colour–colour diagram of the SQM minus V_j Johnson band versus the Johnson B_j minus V_j colour index for different spectra of typical street lights. The right scale of the figure is offset by 0.35 mag from the left scale, because of a hardware offset associated with the SQM (Cinzano 2005). The red stars correspond to low-pressure sodium lamps, pure amber LEDs and others; the black down-pointing triangles are standard high-pressure sodium lamps; the yellow left-pointing triangles are high-pressure lamps without Hg, high-pressure lamps with phosphor, very warm ceramic metal halide and PC-amber lamps (CCT < 2200 K); the green squares correspond to mercury lamps; the cyan circles correspond to warm white LEDs (CCT 2200–3500 K) and normal warm ceramic metal halide; the blue right-pointing triangles correspond to cool white LEDs (CCT 3500–9000 K), standard metal halide and ceramic metal halide. The error bars correspond to the most extreme values of each category. [A colour version of this figure is available in the online version.]

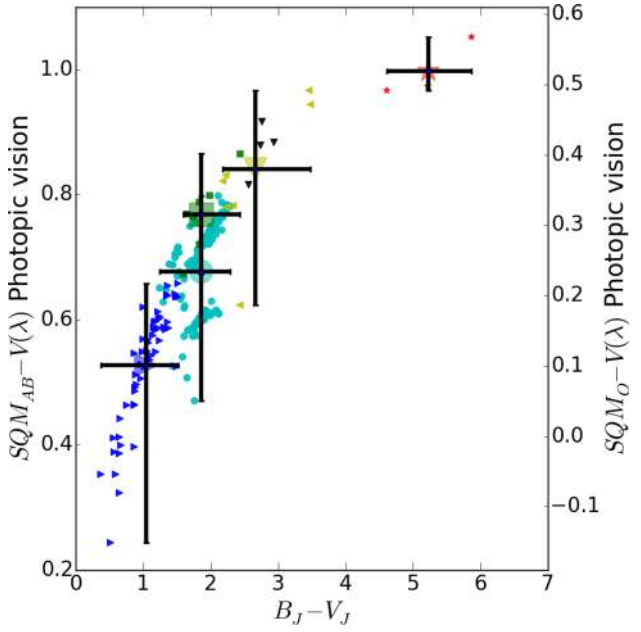

Figure 6. Colour–colour diagram of the $SQM - V(\lambda)$ CIE 1931 photopic curve versus the colour Johnson $B_j - V_j$ for different spectra of typical street lights. Same colour code and symbols as in Fig. 5.

In order to show the systematic differences in this section, we are going to compare the different results the SQM gives when it receives direct light from sample street lights and also compare these results with the real problem that the SQM would ideally solve, which is the stars' visibility for humans.

In Fig. 5, we can see how $SQM_{\rm AB} - V_j$ depends on the B_j–V_j colour. Excluding the effect of the natural spectrum of the sky (i.e. the case in which the sky brightness is dominated by light pollution), ignoring the lamp spectra results in a span of values as large as 0.55 mag along the $SQM_{\rm AB} - V_j$ axis (∼0.25 to ∼0.8). Even if we know the technology of the lamp (e.g. as illustrated by the symbols in Fig. 5), we observe a large span of $SQM_{\rm AB} - V_j$ values for the same technology class. The span of $SQM_{\rm AB} - V_j$ values can increase up to 0.35 mag for lamps that include more blue light (blue right-pointing triangles in Fig. 5), 0.32 mag for whitish lamps (cyan circles in Fig. 5) and even 0.25 mag for yellowish lamps (yellow left-pointing triangles in Fig. 5). Almost all the lamps are concentrated in the region $SQM_{\rm AB} - V_j = 0.55 \pm 0.20$.

It is possible to see that there is an important difference between Figs 5 and 6. The latter shows the $SQM_{\rm AB} - V(\lambda)$ colour diagram. Indeed, the dispersion of values along the vertical axis is larger when expressed with the $V(\lambda)$ curve compared with use of the V Johnson band (0.72 versus 0.55). It is also interesting to see that, for the category of white lamps (cyan circles), the lamp population appears to be split into two subclasses in both figures. Another striking feature of the plots is the important differences in vertical axis values between each technology/colour. There is also a systematic offset in the vertical axis values between the two plots. For greenish lamps, we have an offset of 0.05, while it is 0.15 with whitish lamps, i.e. the higher values obtained in Fig. 6.

The SQM has a spectral sensitivity that is in between the B_j and V_j bands. It is assumed by the manufacturer that it is a better tracer of scotopic vision than the V_j band. It is noticeable from Fig. 6 that, if one does not know the kind of lamp/colour, an error as large as 1.2 mag can be made when using SQM to estimate the scotopic magnitude $V(\lambda)$. With the SQM, the sky appears brighter for reddish lamps in comparison with the photopic perception.

Fig. 7, which gives the SQM reading in reference to the scotopic system, shows that the relationship goes in the opposite direction from that in Fig. 6. The figure shows that if we use the SQM to evaluate perception in the scotopic regime, the sky appears darker for reddish lamps. The large dispersion of sodium-like lamps is noticeable in Fig. 7, with more than 0.2 mag of dispersion. Figs 6 and 7 show clear correlations with the $B_j - V_j$ colour index. This means that it is more accurate to measure the colour to estimate $SQM - V(\lambda)$ or $SQM - V'(\lambda)$ than to just guess it from a technology-based averaged value. In other words, if a correction is going to be made to the SQM readings, to consider the technology of the lamp is not accurate enough, but using the $B_j - V_j$ colour it is possible to correct the measurements of an SQM properly. Therefore, if using a colour-sensitive instrument like a digital single-lens reflex camera (DSLR) is possible, to obtain an estimation of the typical $B_j - V_j$ colour of the light pollution of a place, an accurate correction can be applied, although a lot of scatter will remain.

On the light-polluted site of the Universidad Complutense de Madrid (UCM) observatory (40°27′04″N, 03°43′34″W), where we can have a sky brightness measurement in clear conditions of $SQM_{\rm O}$ = 18, the light pollution was originally dominated by HPS lamps,

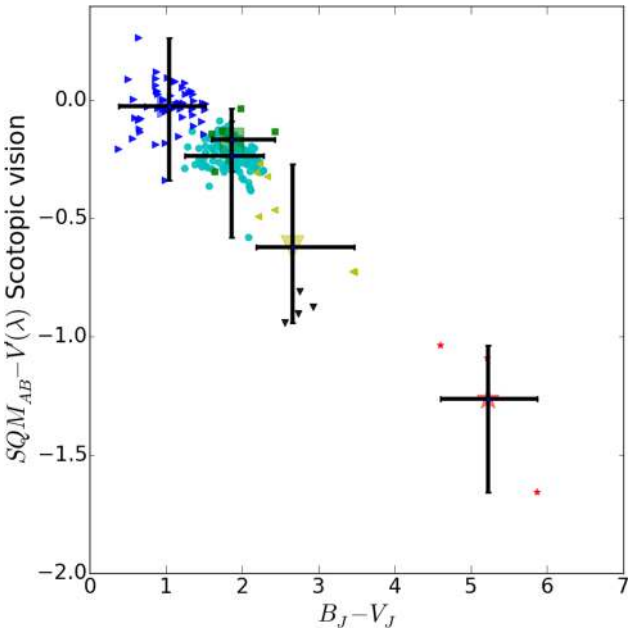

Figure 7. Colour–colour diagram of $SQM - V'(\lambda)$ CIE 1951 scotopic vision versus the colour index $B_j - V_j$ for different spectra of typical street lights. In this Figure there is no offset between the calculated and instrumental magnitudes. Same colour code and symbols as in Fig. 5.

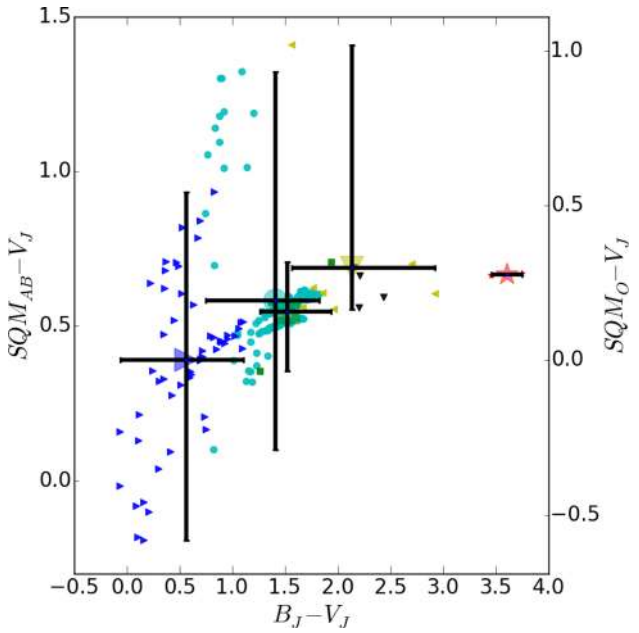

Figure 8. Colour–colour diagram of $SQM - V_j$ Johnson band versus Johnson $B_j - V_j$ colour index for different spectra of typical street lights scattered by the atmosphere at 3 km. The right scale of the figure is offset by 0.35 mag from the left scale, because of a hardware offset associated with the SQM (Cinzano 2005). The red stars correspond to low-pressure sodium lamps, pure amber LEDs and others; the black down-pointing triangles are standard high-pressure sodium lamps; the yellow left-pointing triangles are high-pressure lamps without Hg, high-pressure lamps with phosphor, very warm ceramic metal halide and PC-amber lamps; the green squares correspond to mercury lamps and cyan circles to warm white LEDs and normal warm ceramic metal halide; the blue right-pointing triangles correspond to cool white LEDs, standard metal halide and ceramic metal halide. The error bars correspond to the most extreme values of each category.

so that the photopic magnitude was 17.15 $(18 - 0.85)$[2] but the scotopic magnitude was 18.6 $(18 + 0.6)$. Since then, the street lights have been gradually changed to blueish lights, but the SQM measurements have still maintained the same readings. The new photopic magnitude assuming pure blueish lamps should be 17.5 $(18 - 0.5)$, so it should look darker than before, but with adapted vision we get a scotopic magnitude of 18 $(18 + 0)$, so it should look brighter. We need to be aware of this effect when we are trying to track the final visual perception of the sky brightness.

2.1.1 Simulation of SQM readings of a realistic sky spectrum

In the previous subsection, we have shown how the SQM readings can be compared with the direct incident light from lamps. A realistic simulation of the SQM response to a variety of spectra needs to take into consideration several factors, for example the contribution of the natural sky, Rayleigh and Mie scattering by air molecules and aerosols. Therefore, to simulate a more realistic scenario, we have added the scattered light from different lamp spectra at various distances (3,[3] 6, 15, 30, 60 and 100 km). Also, we applied the Kocifaj model (MNRAS: Aubé & Kocifaj 2012) using the constants from Aubé, Roby & Kocifaj (2013) and combined this with natural component spectra from the Montsec Observatory acquired with the Spectrophotometer for Aerosol Night Detection (SAND) spectrograph.

In both Figs 5 and 8, a comparison is made between the SQM and *V* Johnson colour and the *B* Johnson and *V* Johnson colour of the street lamp spectrum. Fig. 8 concerns scattered light produced by a large city at a distance of 3 km and Fig. 5 concerns direct light. The data show clearly that, when light sources have a redder colour, the scattering does not cause a significant change between the SQM band readings and the *V* Johnson band values. In the same two figures, it becomes evident that bluer coloured lamps cause two significant changes. First, lamps with significant infrared emission have a completely different behaviour from pure visible light emission, due to the low atmospheric scattering in the infrared. Secondly, in Fig. 5 the colour difference between the redder and bluer lamps is ∼0.5 mag, while in Fig. 8 this has increased to ∼0.7 mag. It is important to mention that in Fig. 8 the more extreme values up to 1.5 mag are not caused by redder or bluer lights, but by lamps with more infrared emission as well as bluer lamps without infrared emission.

The comparison between Figs 6 and 9 is a similar case to the comparison between Figs 5 and 8. Fig. 10 depicts a different situation, as the data of SQM readings against scotopic magnitudes do not diverge from one another. Although the data in Fig. 10 are more dispersed, this figure still leads to the same conclusion as Fig. 7: mainly that lamps with bluer light cause more sky brightness than lamps with redder light. It is important to highlight that, unlike lamps with yellower lights, all lamps with white lights, including LEDs and regardless of their technology, systematically create brighter skies by 0.4 mag according to the SQM readings. Keep in mind that SQM readings vary from actual scotopic vision, even if for cool lamps they produce the right values, because the SQM is unable to detect variations in colour and this may lead to misinterpretations.

[2] These values should be read as sky brightness in the band ($SQM_O \pm$ correction).
[3] City edge.

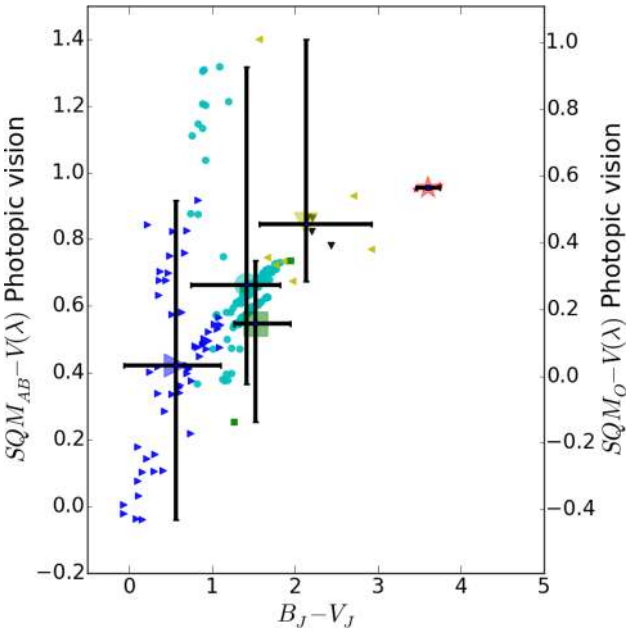

Figure 9. Colour–colour diagram of the $SQM - V(\lambda)$ CIE 1931 photopic curve versus the colour Johnson $B_j - V_j$ for different spectra of sky polluted by at 3 km of the source by typical street lights. Same colour code and symbols as in Fig. 5.

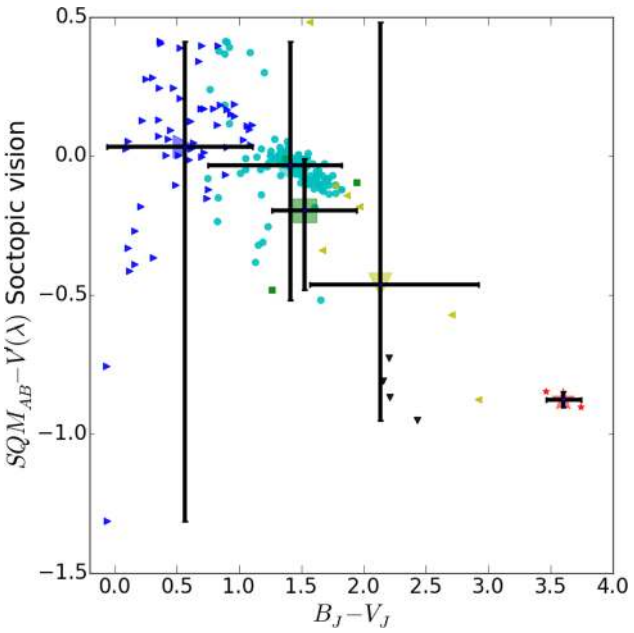

Figure 10. Colour–colour diagram of $SQM - V'(\lambda)$ CIE 1951 scotopic vision versus the colour index $B_j - V_j$ for different spectra of sky polluted by at 3 km of the source by typical street lights (city edge). In this case, there is no offset between the calculated and instrumental magnitudes. Same colour code and symbols as in Fig. 5.

3 EFFECT OF DIFERENT ILLUMINATION TECHNOLOGIES ON SKY BRIGHTNESS AND ITS IMPACT ON SQM MONITORING

As we explained in the Introduction, we are living during a time of revolution when it comes to illumination technology. With synthetic photometry, we are able to simulate how the scattering and spectra

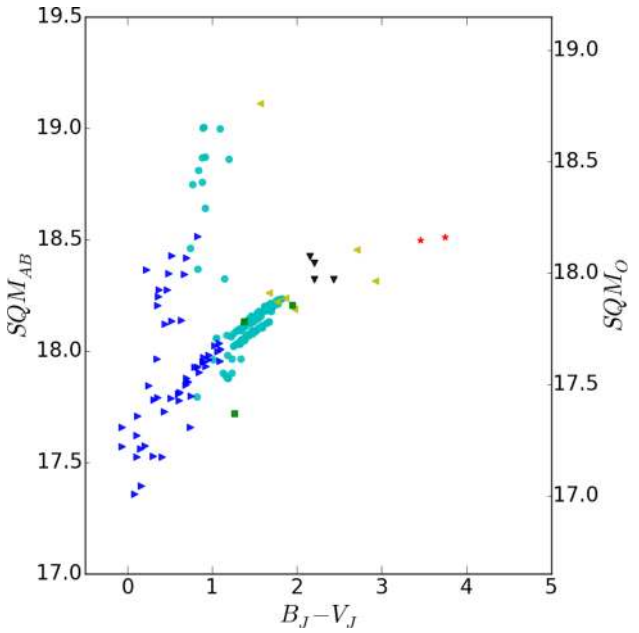

Figure 11. SQM readings simulation from a realistic polluted sky by at 3 km of the source by typical street lights. Same colour code and symbols as in Fig. 5.

of new lighting systems impact sky brightness. Similarly to our method in the previous section, we created a realistic simulation of the sky spectrum. In the experiment we will be discussing now, we have normalized the spectra to the same lumens emission before applying the scattering process and adding the natural component. In Fig. 11 we see that, for the same lumens, bluer lamps create much brighter SQM readings, but, even so, we have to keep in mind that the SQM is not giving us the right scotopic magnitudes. Therefore, if we measure a SB of $SQM_{\rm O} = 18.2$ in a high-pressure sodium-dominant place at 3 km distance from the main source, the real scotopic brightness is 19 according to Fig. 9. If the illumination is changed suddenly to a bluer LED, our SQM will measure $SQM_{\rm O} =$ 17–17.5 and the scotopic magnitude will remain the same. This means that, according to the SQM readings, we obtained a brighter sky by 0.7–1.2 mag, but in reality we obtain a brighter sky by 1.5–2 mag for human eyes when we change from orange light to white light with a content of blue light.

This effect is less pronounced when we go further away from the source: the absorption of blue light means that yellowish light can go further. This explains why, in Fig. 12, the SQM readings of 0.4 mag are lower than before. The new illumination technologies are impacting the zenith and this affects the SQM readings. When we compared old illumination technologies with new illumination technologies and combined both with a fixed amount of light emitted into the atmosphere as well as fixed illumination levels, we were able to conclude that the newer illumination technology with more blue content creates brighter skies. Even in the case in Kolláth et al. (2016), where the previous street lighting had large Upper Light Output Ratio (ULOR) and no blocking effect, the new illumination compensates for the better photometry owing to the more contaminant effect of blue light.

This example shows how, even in places far removed from the polluting source, the effect of a change of illumination is still significant when it concerns SQM readings. This visible effect is easier to observe when the light pollution is stronger. The real effects of the two methods currently used to reduce both light emission into the upper

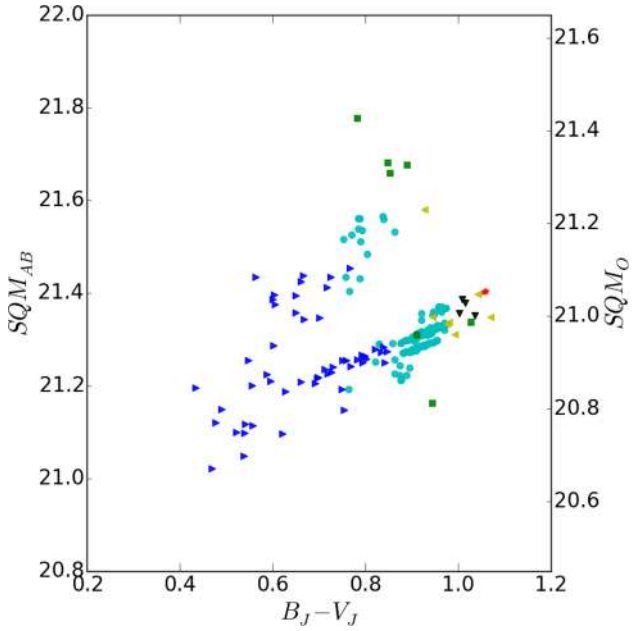

Figure 12. SQM readings simulation from a realistic polluted sky by at 60 km of the source by typical street lights. Same colour code and symbols as in Fig. 5.

hemisphere and the illumination levels of new LED lighting systems cannot be simulated fully in this article, because of their complexity. The main goal of this article is to create awareness in SQM users and to inform them that, when the SQM readings are lower due to less light emitted upwards or lower illumination levels, this does not necessarily mean that the sky brightness quality has improved. In reality, the sky brightness quality may even have deteriorated. It is therefore vital that the effect of the SQM spectral response, as explained in this article, should be considered before interpreting low SQM readings. To help with future diagnostics of SQM data, we have created an extra sample of simulations that can be found as additional information to this article.

3.1 Application to a practical case: Madrid and Milan

In order to reduce energy consumption and light pollution, the city of Madrid has recently replaced most of its midsize high-pressure sodium street lamps with LED 3000 K lamps. These midsize street lamps account for 40 per cent of the total amount of street lamps in the city. There is a current plan to replace the remaining 60 per cent of street lamps sometime in the near future. Meanwhile, the city of Milan has recently replaced its old street lights with LED lamps of 4000 K. But are these new lamps really reducing light pollution, as has been claimed?

In Table 1, it is evident that the new replacement lamps increase the sky brightness for adapted human vision by 1.04 mag in the case of the 3000 K lamps and 1.25 mag in the case of 4000 K lamps. On a linear scale, the sky brightness for the LED 3000 K increases by 161 per cent and that for the LED 4000 K by 216 per cent.

The current retrofits, both in Madrid and Milan, are focusing solely on replacing the lamp and not the full illumination system. The most typical street luminaire used on the roads of Madrid is the cobra head with 5 per cent ULOR, but there are alternative luminaires available that emit 0 per cent ULOR. The next model considers the light emitted upwards and the horizontal emission that is blocked by surrounding buildings. It does not take into account any other objects that may block emission, such as trees. Also, in this section we will refer to the real sky brightness as the sky seen by a human with scotopic vision, because it is the kind of vision that the humans really use to observe the sky.

When we change not only the lamps but also the luminaire to a type that emits 0 per cent ULOR, the light emission towards the street will automatically increase. As a result, the energy output can be decreased to compensate for this emission increase, thus saving on energy consumption. If the albedo value of the ground was 0.2, for example, the new total emission towards the sky would be just 80 per cent of the current emission.

If the city of Madrid were to change the current luminaires, the new luminaries would have 0 per cent ULOR, combined with the new LED 3000 K lamps. Would this reduce light pollution? And how accurately would Madrid's SQM station be able to measure these changes? As was discussed earlier in this article, the SQM is unable to track real adapted human vision and this means that SQM readings do not always reflect reality. For example, in the case of the 3000 K lamp, the SQM will indicate no increase of sky brightness (SQM band) when in reality there is an increase of 111 per cent and in the case of the 4000 K lamps, the SQM will indicate an increase of 14 per cent (SQM band) when in reality it is 153 per cent.

In the case of Madrid, the emission of the LEDs can be easily adjusted with a regulation system. If the possibility of regulating the emission down to 60 per cent of the original illumination level is combined with the use of luminaires of 0 per cent ULOR, the 3000 K

Table 1. This table summarizes the results of the predicted sky brightess in three observation bands: photopic, scotopic and SQM. This simulation considers the sky brightness measured at 3 km from the centre of a city like Madrid (city edge). Also is included as reference is the change of signal that each band will receive on a linear scale relative to a sodium high-pressure lamp with 5 per cent. In the last four cases, the light emission levels (amount of lumens needed to produce a given illumination level) have been reduced to try to find the 'break even' point where the blue light effect is compensated by reduction of the illumination level.

Lamp	SQM (mag)	SQM	Photo (mag)	Photo	Scoto (mag)	Scoto
HPS ULOR 5 per cent	18.32	1	17.53	1	19.26	1
LED 3000 K ULOR 5 per cent	18.15	1.17	17.49	1.04	18.22	2.61
LED 4000 K ULOR 5 per cent	17.95	1.41	17.46	1.07	18.01	3.16
LED 3000 K ULOR 0 per cent	18.39	0.94	17.73	0.83	18.45	2.11
LED 4000 K ULOR 0 per cent	18.18	1.14	17.71	0.86	18.25	2.54
LED 3000 K ULOR 0 per cent L. Level 60 per cent	18.95	0.56	18.25	0.52	18.98	1.29
LED 4000 K ULOR 0 per cent L. Level 60 per cent	18.71	0.69	18.23	0.52	18.78	1.56
LED 3000 K ULOR 0 per cent L. Level 42 per cent	19.41	0.37	18.74	0.33	19.43	0.86
LED 4000 K ULOR 0 per cent L. Level 42 per cent	19.22	0.44	18.74	0.33	19.27	0.99

lamps would appear to have a 45 per cent reduction according to the SQM, but in reality there is an emission increase of 29 per cent. In the case of the 4000 K lamps, the SQM would show a reduction of 30 per cent when in reality there is an emission increase by 56 per cent.

We can conclude from the previously discussed measurements that light pollution has increased due to the new LED lamps. With current numbers, it is safe to say that 3000 K and 4000 K lamps would only reduce light pollution if they were to be switched off or dimmed down to an extremely low intensity. To be more specific, if changing HPS lamps to LED 3000 K lamps were meant to reduce light pollution, it would be necessary to reduce street illumination to below 42 per cent of the original level. Such low illumination levels could cause certain streets and places to become so dark that citizens would no longer experience a sense of safety and security. This happened in Madrid, according to the Madrid city council. That is why 60 per cent is the dimmest level used in Madrid nowadays. This claim is not shared by scientific community, but nevertheless is commonly used by technicians.

4 DATA BIAS FROM THE BROAD-BAND SENSITIVITY OF THE SQM

The spectral composition of night-sky light varies with the meteorological conditions and typically undergoes large changes during the passage of a front, but it can also appear unstable in a developing air mass or even in calm air, due to fluctuations in the local aerosol system. Turbulent mixing, rising humidity, a change in the direction of the wind or the surrounding terrain, as well as the origin of the air mass, have a direct impact on the actual optical properties of the aerosol (Bukowiecki et al. 2002), which, in turn, modifies the light field near the ground. Light emissions from ground-based sources predetermine the spectral properties of diffuse light. However, aerosols, dust particles, water droplets and other atmospheric constituents change this picture, depending on the weighted contributions of the individual atmospheric components. For instance, maritime aerosol is dominated by water or sea salt, both being slightly absorbing or non-absorbing materials, while urban aerosol typically originates from anthropogenic sources and thus may contain carbonaceous species. Therefore, maritime aerosols can act as efficient scatterers and thus intensify the night-sky radiance. In contrast, urban aerosols may cause an intensity decay, due to enhanced absorption of upward light emissions. The total effect of aerosol particles is often parametrized through the Ångström exponent, α (see e.g. Esposito, Pavese & Serio 2001), which is used to model the spectral behaviour of the aerosol optical depth (AOD):

$$AOD(\lambda) = AOD(500)\left(\frac{\lambda}{500}\right)^{-\alpha}. \quad (6)$$

The wavelength λ introduced above is measured in nanometres (nm). Cachorro et al. (2000) have shown that α can range from -0.5 to more than 2, while Rayleigh theory dictates that the optical depth of the gaseous constituents (excluding absorption) is proportional to $\lambda^{-4.09}$ (Fröhlich & Shaw 1980). To make things even more complex, a cloud layer has rather a neutral effect on the initial spectra, because the water droplets dispersed in the clouds are large enough to scatter in the geometrical optics regime.

The above effects combine with the average spectral sensitivity of the SQM device, $T(\lambda)$, thus the signal recorded at the ground is

$$S_{SQM} = \int_{\lambda 1}^{\lambda 2} T(\lambda)\,\phi_0(\lambda)\,\mathrm{d}\lambda, \quad (7)$$

where ϕ_0 is the initial spectral signal (e.g. the sky radiance) and the integration interval $\lambda_1 \rightarrow \lambda_2$ covers the SQM operating wavelengths. It has been shown by Cinzano (2005) that $T(\lambda)$ varies with the angle of incidence of the beam, θ, and thus a general functional form for $T(\theta, \lambda)$ should be considered in data processing, except for e.g. SQM-L, which has a small field of view (Cinzano 2007). As a consequence, the error margin of the approximation $T(\theta, \lambda) \rightarrow T(\lambda)$ is expected to be low for an SQM-L device.

4.1 Lamp spectral distributions considered in this research

The Lamp Spectral Power Distribution Database (LSPDD) is available online[4] and is maintained by the Light Pollution Group of Cégep de Sherbrooke. This dataset aims to provide independent information about the spectral characteristics of commercial lamp products. Each lamp has its associated datasheet providing the lamp's characteristics, like the spectral power distribution (SPD), correlated colour temperature, percentage of blue light and the impact indices introduced in Aubé et al. (2013). The LSPDD distributes SPDs in ASCII text format (273–900 nm, every 0.5 nm), allowing any other researcher to easily use the data for their own research. The LSPDD is released under the Creative Commons BY-NC-ND license. The data file is available in each lamp datasheet. All the SPD data are measured with the same spectrometer model (the Black Comet model from Stellarnet Inc.), factory calibrated according to National Institute of Standards and Technology (NIST).

An example of the SPD for a white LED with $CCT \simeq 4000$ K from the LSPDD dataset and a screenshot of the web interface is shown in Fig. 13.

The LSPDD is based mainly on lab tests and on new lamps. However, many of the lamps change their spectra with time, therefore we have also used the Laboratorio de Instrumentación Científica Avanzada (LICA)-UCM (Tapia Ayuga, Sánchez de Miguel & Zamorano Calvo 2015), because it is based on street measurements. All the spectra used are normalized to equal luminance on the pavement surface.

4.2 Effect of SQM spectral sensitivity on cloud brightening factor measurements

It has been pointed out in previous sections that the spectral sensitivity of a SQM device combines with atmospheric optical effects, while both form an output signal that is consequently used to characterize the diffuse light of a night sky. A synergy effect is a distortion of the original spectra, which makes the data interpretation partly uncertain. The light beams emitted from distant parts of an urban area propagate over longer optical paths and are attenuated (and scattered) more efficiently than those emitted from illumination elements surrounding the measuring point. The zenith spectral radiance can therefore change with position even if the measurements are made within the territory of a city. The same is true for overcast skies. The brightening factor may vary with time and position and of course with wavelength (Aubé et al. 2016).

In order to simulate this effect, we can use synthetic photometry, explained in Section 2, and we only need to multiply our source spectrum by the amplification monochromatic curve of Aubé et al. (2016). A typical result is shown in Fig. 14, in which SQM_{CB} is the SQM reading with the SQM under a cloudy sky and the original measurements without clouds are denoted by *SQM*.

[4] www.lspdd.com

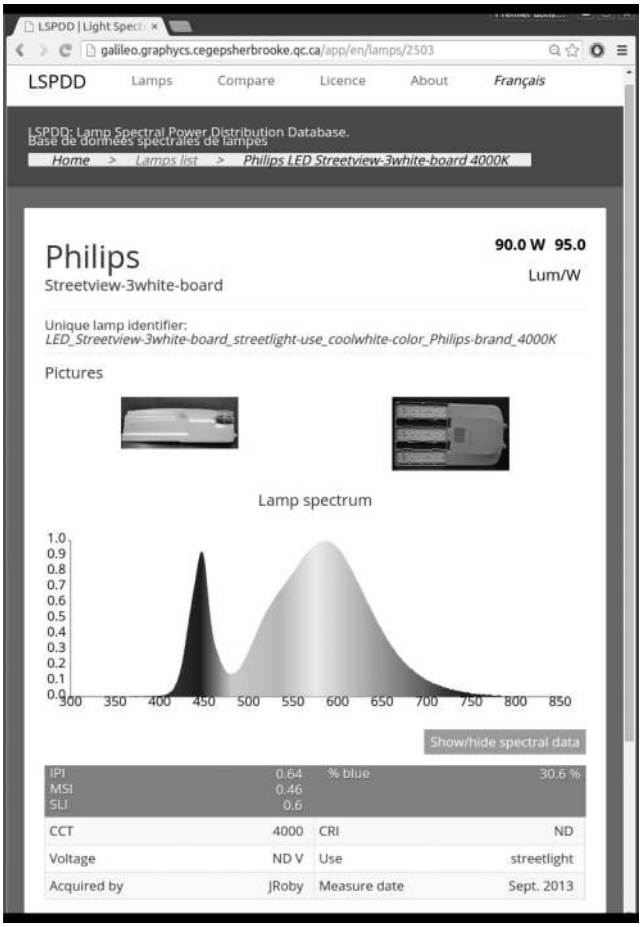

Figure 13. Screenshot of the web interface of the LSPDD. This window shows an example of a Philips LED 4000 K street light.

The SQM reading sensitivity drops quickly for wavelengths above 600 nm, thus the sky appears artificially dimmer for these wavelengths. The effects of reddening are difficult to identify because the spectral response of the SQM is higher at short wavelengths. This is why the measured amplification factors (AF) tend to be lower than those numerically computed for the whole visible spectrum (see Fig. 15). Namely, the theoretical values of AF increase steeply from blue to red, but the normalized response of the SQM is far below unity at wavelengths above 600 nm.

Fig. 15 shows how the cloud AF varys with the lighting technology and, in turn, the colour of the lamps. This plot is for the specific case of a stratus cloud with cloud base height of 500 m and a low aerosol loading characterized by an AOD of 0.1 in all cases. The lamp upward light output ratio (ULOR) was set to 5 per cent. The line is the theoretical monochromatic amplification calculated by Aubé et al. (2016). The wavelength associated with each lamp (points in the figure) corresponds to the average emission wavelength of the lamp. The average emission wavelength is calculated using equation (3), where $T(\lambda)$ must be replaced by $\phi(\lambda)$, the emission spectrum of the lamp. This plot shows that the SQM amplification factor is higher for redder lamps. The large point with error bars corresponds to the maximum emission wavelength of the averaged spectrum of all lamps in a given lamp group or technology. In summary, this plot shows that the observed amplification factor when using an SQM is underestimated by about 10 per cent for most of the lamps, but this percentage depends strongly

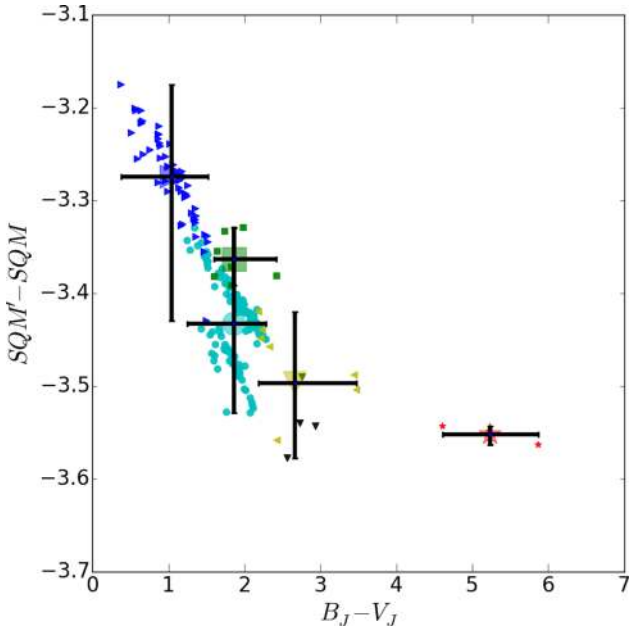

Figure 14. Change of the cloud brightening factor in synthetic photometry (see Section 2), where SQM' represents the SQM reading with clouds, and SQM that without clouds. This differential amplification is compared with the colour index $B_j - V_j$ in order to distinguish the different lighting technologies. The error bars represent the maximum range of possible values in each lamp category according to the SPD data available. This plot is for stratus clouds with cloud base height of 0.5 km, street lights with 5 per cent ULOR and an AOD of 0.1.

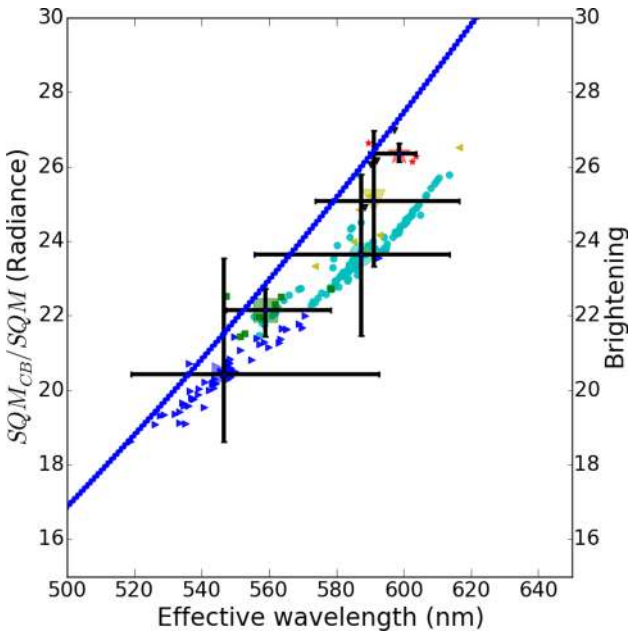

Figure 15. Change in amplification by the clouds in synthetic photometry (see Section 2), where SQM_{CB} represents the SQM reading with clouds, and SQM that without clouds. Same plot as Fig. 14 but, for comparison, the different technologies use the effective wavelength of each spectrum (King 1952). The error bars represent the maximum range of possible values in each lamp category according to the SPD data available. The blue line represents the monochromatic amplification by the clouds; to interpret this curve, use the right axis. The amplification factors are for stratus clouds with cloud base height of 0.5 km, street lights with 5 per cent ULOR and an AOD of 0.1.

on the specific lamp used. This effect is produced mainly for the non-monochromatic emission of these lamps.

4.3 Effect of natural sources on SQM readings

In this section, we evaluate the impact of having different natural sources entering the field of view (FOV) of the SQM. The impact of each source is driven by both the angular sensitivity curve and the spectral response. In this article, we choose to focus mainly on the spectral response effect.

4.3.1 Effect of the field of view angular sensitivity

Another source of error may be the natural sources of light present in the SQM field of view. By way of example, we have made an analysis of the effect of the Moon on the measurements of a SQM.

We characterized the SQM FOV used for this study as shown in Fig. 1. The sensitivity drops very rapidly with angle, but if a very bright source lies at a large angle, it can contribute significantly to the total signal measured, even if the sensitivity is very low at that angle. As an example, we will estimate the impact of the full Moon at 50° elevation, i.e. at 40° from the centre of the FOV. The sensitivity at that angle is ∼1 per cent of the central value. Assuming a Moon magnitude of −12.74 (Williams 2010), when attenuated to 1 per cent (+5 magnitude) it gives an equivalent magnitude of −7.74. In other words, having the Moon at 40° produces the same signal at the SQM as having an object of mag −7.74 at zenith. In highly light polluted cities like Madrid, the SQM zenith sky brightness in very clear sky is around 18.5 mag arcsec^{-2} (Sánchez de Miguel 2015a), while in the most pristine skies it is about 21.9 mag arcsec^{-2} (Benn & Ellison 1998). To get a crude estimate of the comparative order of magnitude between the Moon at 40° and the sky brightness, let us determine the magnitude of the equivalent point source at zenith that would yield the same signal that the SQM reads from the sky. We can calculate the equivalent magnitude of the sky from its surface brightness (mag arcsec^{-2}) with the equation below:

$$m_{SQM} = SB - 2.5 \log \left(\frac{\pi D^2}{4} \right), \quad (8)$$

where SB is the surface brightness in mag arcsec^{-2} and D is the angular FOV of the SQM (FWHM = 20°) in arcsec.

For the Madrid sky, we obtain a magnitude of −5.5, while for a pristine sky the equivalent magnitude is −2.1. This indicates that the difference in magnitude between the direct contribution of the Moon at 50° altitude and the contribution of the moonless sky is $\Delta m = -2.24$ (5.5–7.74) for Madrid and $\Delta m = -5.64$ (2.1–7.74) for a pristine sky. That means that the contribution of the Moon to the SQM radiance at that specific altitude is ∼ eight times larger than the moonless sky brightness in Madrid and ∼175 times larger in pristine skies. Note that this estimate does not consider the contribution of moonlight scattered by the atmosphere into the FOV.

Pun et al. (2014) used a model to evaluate the moonlight scattered to the zenith for many Moon altitudes and Moon phases for a given V-band extinction coefficient of $k = 0.58$ mag airmass^{-1}. In particular, their fig. 7 shows that, at 50° altitude, the contribution of zenith light scattered from the Moon reduces the sky brightness of 21.2 mag arcsec^{-2} (site Astropark Hong Kong) by ∼3.5 mag arcsec^{-2}. If we apply equation (8) to this sky brightness, we obtain an equivalent magnitude of −2.82, which leads to a magnitude difference with an equivalent magnitude of the direct light of the Moon attenuated for the angle of 40° from the FOV centre of $\Delta m = 2.82 - 7.74 = -4.92$. The difference in magnitude between the direct moonlight at 40° of the centre FOV and the scattered moonlight is $\Delta m = 3.5 - 4.92 = -1.42$ mag (i.e. a factor of 3.7 times on a radiance linear scale).

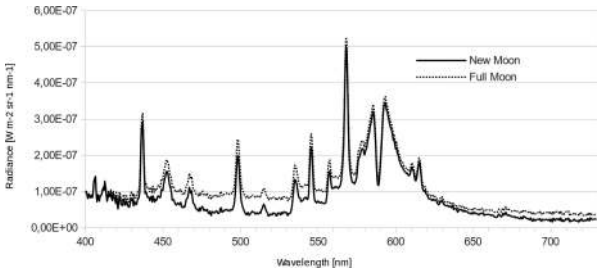

Figure 16. Observed zenith radiance in UCM during new Moon (2015 June 3) and full Moon (2015 June 16) at around 23h50 UTC.

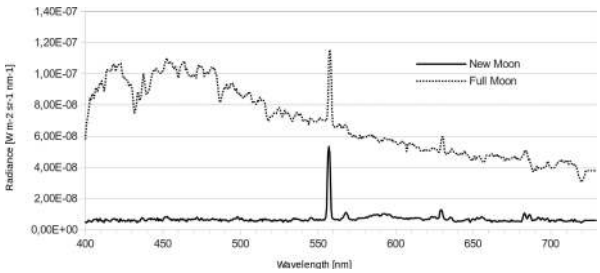

Figure 17. Observed zenith radiance in Montsec during new Moon (2015 June 3) and full Moon (2015 June 16) at around 23h50 UTC.

4.3.2 Effect of the SQM spectral response

The spectral impact of the different natural contributions to zenith SQM readings requires access to a measured spectral database of night-sky radiance. We extracted this information from our archives; it was acquired with the SAND-4 spectrometers (Aubé 2007, 2015) for two extreme sites: an urban site located at UCM and a rural site located in the Montsec astronomical park in Cataluña, Spain (42°01′28″N, 00°44′10″E). We combined information from the different sources present or absent from different spectra (e.g. with or without the Moon). Actually, we used the full Moon night of 2015 June 3–4 and the new Moon night of 2015 June 16–17 (Figs 16 and 17). For both sites, we used data taken around the same time of night (∼23h50) to remove the effect of variation of sky brightness through the night. For the first night, the altitude of the Moon was 27° and the illumination of the Moon 98 per cent, whereas it was 0 per cent for the second night. Among other operations, the SAND-4 analysis software removes the continuous spectrum as its last step. This is done by fitting a low-order polynomial on a set of wavelengths that do not show any contamination from HID lamps, natural airglow or Fraunhofer lines.

We used a multi-Gaussian fitting algorithm to approximate the line spectrum as a combination of many Gaussian lines (actually 30 Gaussian profiles). In that process, we locked the FWHM of the lines to a constant value, so that this parameter is determined by the optics of SAND-4. The retained FWHM for the UCM instrument was 1.5 nm, while it was 1.25 nm for the Montsec instrument. With detailed knowledge of the contribution of the spectral lines to the spectrum, it was then possible to evaluate separately the contribution of lines associated with human activities and the natural airglow. The artificial and natural contributions to the continuous spectrum (e.g. car headlights, halogen and incandescent, LEDs, star

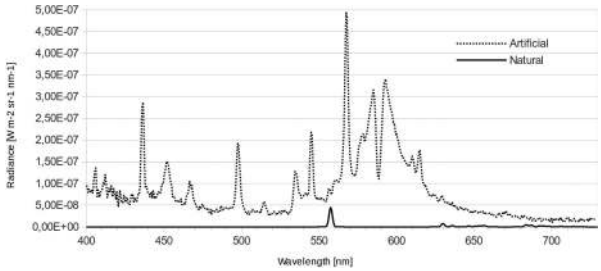

Figure 18. Zenith radiance from artificial and natural airglow in UCM extracted from Figs 16 and 17.

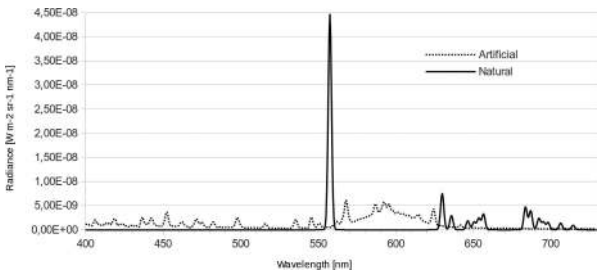

Figure 19. Zenith radiance from artificial and natural airglow in Montsec extracted from Figs 16 and 17.

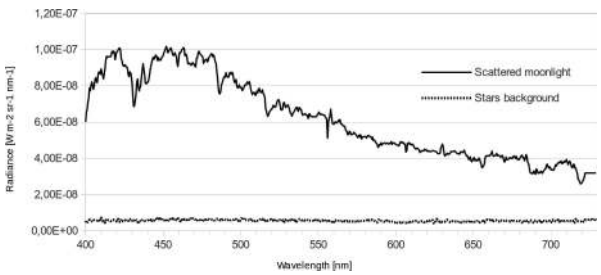

Figure 20. Scattered moonlight and star background zenith radiance extracted from Figs 16 and 17.

background) were obtained by subtracting the spectral lines fitted from the new Moon observations (Figs 18 and 19). To estimate the typical star background contribution, we assumed that the continuous spectrum of the new Moon in Montsec is dominated by the star background (Fig. 20). To estimate the artificial part of the continuous spectrum, we started from the new Moon measurement in Madrid and subtracted the spectral lines fitted along with the star background previously found with the Montsec measurement. Finally, the artificial portion of the continuous spectrum in Montsec was estimated by re-scaling the artificial continuous spectrum found for Madrid using the averaged ratio of the artificial line spectra for the two sites. By doing this, we then assumed that the proportion of the artificial line radiance to the artificial continuous radiance is more or less the same for both sites. Lastly, to determine the contribution of the scattered moonlight, we subtracted the new Moon spectrum from the full Moon spectrum (Fig. 20). Note that we took care to acquire the spectrum at the same time of night for both nights, to exclude the effect of the decrease in light levels through the night. At the end of that process, we had the following basic spectra: (1) the artificial line and artificial continuous spectrum at UCM; (2) the artificial line and artificial continuous spectrum at Montsec; (3) the natural sky glow; (4) the star background; and (5) the full Moon scattered moonlight at 27° of Moon altitude.

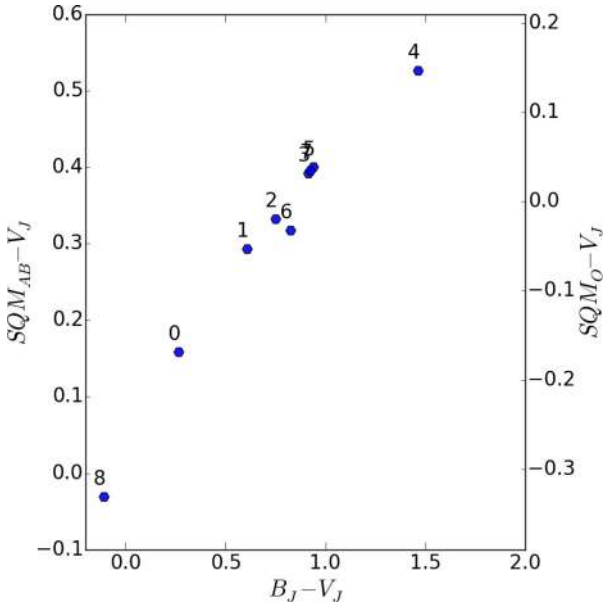

Figure 21. $SQM - V_j$ colour versus $B_j - V_j$ colour for different sky radiance components, where $0 = A + N + S + SM$ in Montsec, 1 is $A + N + S + SM$ in UCM, 2 is $A + N + S$ in Montsec, 3 is $A + N + S$ in UCM, 4 is $A + N$ in Montsec, 5 is $A + N$ in UCM, 6 is A in Montsec, 7 is A in UCM, 8 = Vega spectrum. Legend: A = artificial radiance, N = natural sky lines radiance, S = star background radiance, SM = scattered moonlight.

The objective when measuring the sky brightness of a given site is in most cases to follow up with a determination of the artificial contribution to the sky brightness. However, it is not obvious how to know what fraction of the SQM measurement is really of human origin. To get a good idea of this, we combine the basic spectra to mimic realistic situations and compare this with what the SQM should detect without any natural sky brightness (i.e. only the artificial brightness). The retained combinations are as follows: (1) artificial and natural airglow spectrum; (2) artificial, natural airglow and star background; and (3) artificial, natural airglow, star background and full Moon scattered moonlight at 27° of Moon altitude. Table 2 shows the shift in sky brightness (mag_{SQM} arcsec^{-2}) of the retained combination in relation to the artificial SB alone. To retrieve the artificial SB from the measured SQM SB, one must add ΔSB to the SQM measurement. The table also indicates the percentage increase in observed radiance compared with the artificial radiance for the given source combination and site. If one wants to determine the percentage of a specific natural source, it is possible to substract 'added to artificial per cent' from the previous line in the table. As an example, if one wants to know the percentage contribution from stars, it is given, in the case of Madrid, by 7 per cent − 0.7 per cent = 6.3 per cent. We can see that, for an urban site like Madrid, the natural airglow contribution to the SQM radiance is very weak (less than 1 per cent). Fig. 21 shows the $SQM - V_j$ colour versus $B_j - V_j$ colour diagram for different sky radiance components as listed in Table 2 for Madrid and Montsec. Even the star background contribution is relatively small (less than 10 per cent) but, as expected, the full Moon contribution is more important: actually, almost as much as the artificial radiance itself (83 per cent − 7 per cent − 0.7 per cent ≃ 75 per cent). The results are completely different for a dark site like Montsec. In such a case, the natural airglow is approximately half the radiance of artificial origin. The star background in that case is approximately four times

Table 2. Impact of natural sources on the SQM measurement in comparison with a pure artificial sky brightness under clear-sky conditions.

Site	Madrid		Montsec	
	ΔSB mag arcsec^{-2}	added to artificial per cent	ΔSB mag arcsec^{-2}	added to artificial per cent
Artificial + natural	+0.007	0.7	+0.43	49
Artificial + natural + stars	+0.07	7	+1.90	475
Artificial + natural + stars + full Moon scat. light	+0.66	83	+4.42	5760

the artificial radiance (475 per cent − 49 per cent ≃ 400 per cent). Finally, it is not surprising to see that the scattered radiance of the full Moon is very high compared with the artificial radiance (∼50 times, i.e. 5760 per cent − 475 per cent − 49 per cent ≃ 5200 per cent).

5 DISCUSSION

SQM photometers have become the reference instrument for measuring night-sky brightness and networks of fixed stations are being built to monitor the evolution of sky brightness. Due to the single broad band (monochannel) of the SQM, eventual lower SQM readings will not necessarily translate to proof that the sources of light pollution that produce less signal on the SQM that the others that produce more signal, really reduce the light pollution (see Table 1).

Our cities are experiencing a change in their artificial illumination, in both intensity and technology. This results in a different colour of the night sky or, more precisely, different night-sky spectra. We have shown that the usual photometric method for correcting from colour using colour terms or magnitude offsets according to the type of lamp is imprecise, due to the large scatter in colour among each lamp type.

To be on the safe side, we recommend using error bars based on the lighting technology instead of a colour-corrected version when the spectra, intensities and proportions of the light pollution sources are unknown.

It is interesting to note that the massive replacement of street illumination with white LEDs will result in darker SQM readings. Also, in the case of photopic vision the sky will appear darker due to the important blue component in LEDs spectra. However the resulting sky is brighter for human-eye scotopic vision for the same radiance.

Does this mean that the SQM should not be used? As long as an improved device is not yet available, we should continue with the SQM. However, we need to train ourselves to avoid interpretation errors in the data and use it only as complementary data to colour-sensitive sensors. Another option is to start using astronomical filters, as has already been done by Kyba et al. (2012).

The SQM is the first device that has been able to measure massive spread and it continues to be a valuable instrument for tracing variations, as long as the spectra of the sources do not undergo extreme changes. Nonetheless, it has become clear that the colour of light should be regarded as a key parameter in light pollution studies. Therefore, the use of colour-sensitive devices should be promoted, especially in places where the light spectra are undergoing changes (Spoelstra 2014; Zamorano et al. 2015). The data already acquired with SQMs are scientifically valid, as is shown in Falchi et al. (2016). However, as is explained in this article and also in Falchi et al. (2016), the lack of colour information with the use of satellites and the SQM might be hiding an increase in light pollution: an increase that, in extreme cases, can be as high as 261 per cent.

6 CONCLUSIONS

Monitoring light pollution levels has become important in the last decades because of rapid industrialization and modernization, especially in densely populated regions. Undoubtedly, the light emissions upwards and the spatial extent of light pollution are both increasing functions of the amount of light emitted and the number of sources. However, an overillumination of the environment is also somehow correlated with population growth, thus optical methods of detection are a desirable technology for watching the effects caused by atmosphere and/or ground-based light sources. Optical methods are preferred because such technology is rapid, the components are inexpensive and the techniques can be automated.

The Sky Quality Meter (SQM) is a widely available device that works properly in the low-intensity regime. Although the SQM is cheap enough and operated worldwide, the data are far from being error-free. Specifically, the SQM has a fast readout and an acceptable dynamic range, but low angular and spectral resolution. This has a direct impact on the interpretation and comparison of light pollution levels measured under distinct conditions. Note that lighting technologies and lamp installations may deviate significantly from case to case. As a result, the same SQM signals might not necessarily mean the same levels of light pollution, because the former can originate from arbitrarily weighted contributions of different lamp types. In addition, atmospheric optics makes things more difficult, mainly due to the non-trivial distortion of optical signals when travelling along different trajectories. In addressing this task, we have become aware of how little we know of the underlying physics and variability of SQM signals.

This article addresses this shortcoming directly and is aimed at a correct understanding of the observed data. It was shown that the blue light emitted abundantly from artificial sources makes the sky colour brighter, thanks to low-intensity light vision (scotopic vision), while the source itself appears darker because it is subject to photopic vision. The latter is also applicable to the *V* band. We have also shown that SQM readings vary with the colour of light pollution sources, but these data can scarcely be predicted as a simple average over the technologies applied. Atmospheric effects impose an additional optical distortion that can change sky colours and even SQM readings. Clouds are recognized as having the greatest influence on the ground-reaching signals, while diffusely reflected light more-or-less mimics the spectrum of artificial sources. This is why the brightening factor (BF) alters with the spectral features of artificial lamps which, in turn, are important sources of uncertainty in SQM readings. This imposes an additional burden on the BF as determined from SQM data, because different effects are involved in forming the zenith radiance under cloudy and cloud-free conditions. There is no doubt that a colour-sensitive device is needed in order to reduce the posible misinterpretation that otherwise arises from SQM data. The SQM is measuring the sky brightness for the

SQM band correctly, but it is not representative of human vision with enough accuracy when the spectra of the sources are more relevant. Such a device can make sky brightness retrieval more accurate and thus more suitable for monitoring optical effects from different installations of ground-based light sources. Although the single measurements of programs like Globe at Night can be very imprecise, amateur measurements are still fundamental to trace the real long-term change of sky quality, as human eye physiology is not expected to change in thousands of years (Kyba et al. 2013; Falchi et al. 2016).

As a final conclusion, the SQM is a good instrument, but not good enough to trace the evolution of the change in sky brightness in a colour-changing world. Colour sensors or multiband cameras are needed to trace the real evolution of sky brightness in this colour-changing world. However, more precise human-based measurements of sky brightness, like the Naked Eye Limiting Magnitude IMO's technique (Rendtel, Arlt & McBeath 1995) and/or Loss of the Night technique (Kyba 2013), are still fundamental to trace the long-term evolution of night sky quality.

ACKNOWLEDGEMENTS

This research was supported by Fonds de recherche du Québec – Nature et technologies (FRQNT-186263) and by the Fédération des Cégeps, by the Slovak Research and Development Agency under contract No. APVV-14-0017, by Spanish projects AYA2012-31277 and AYA2013-46724-P and the Spanish Network for Light Pollution Studies (AYA2015-71542-REDT) from the Spanish Ministerio de Economía y Competitividad. This research also received support from a Medzinárodná Vedecko-Technická Spolupráca (MVTS) grant of the Slovak Academy of Sciences. This research was supported in part by the STARS4ALL project and ORISON project funded by the European Union H2020-ICT-2015-688135 and H2020-INFRASUPP-2015-2.

We thank A. Morin-Paulhus, a former student from the Cégep de Sherbrooke, who developed the web-based interface of the LSPDD database, along with S. Ribas for the maintenance of the SAND instrument in Montsec. We also thank Emma Rebecca Howard and the referee for their comments.

REFERENCES

Aubé M., 2007, in Proceedings of Starlight 2007 Conference, Light Pollution Modeling and Detection in a Heterogeneous Environment. Starlight Initiative, Instituto de Astrofísica de Canarias (IAC), Santa Curz de Tenerife, Spain

Aubé M., 2015, SAND Project Website. Available at: http://cegepsherbrooke.qc.ca/~aubema/index.php/Prof/SandEn

Aubé M., Kocifaj M., 2012, MNRAS, 422, 819

Aubé M., Roby J., Kocifaj M., 2013, PloS One, 8, e67798

Aubé M., Kocifaj M., Zamorano J., Solano Lamphar H. A., Sanchez de Miguel A., 2016, J. Quant. Spectrosc. Radiat. Transfer, 181, 11

Bará S. et al., 2015, Report of the 2014 LoNNe Intercomparison Campaign. Available at: http://eprints.ucm.es/32989/

Benn C., Ellison S., 1998, Technical report, La Palma Tech. Note 115. Isaac Newton Group of Telescopes, La Palma

Biggs J. D., Fouché T., Bilki F., Zadnik M. G., 2012, MNRAS, 421, 1450

Bukowiecki N., Kittelson D., Watts W., Burtscher H., Weingartner E., Baltensperger U., 2002, J. Aerosol Sci., 33, 1139

Cachorro V. E., Durán P., Vergaz R., de Frutos A. M., 2000, J. Aerosol Sci., 31, 687

Cinzano P., 2005, Night Sky Photometry with Sky Quality Meter. Tech. Rep. 9, ISTIL. Available at: http://www.lightpollution.it/download/sqmreport.pdf

Cinzano P., 2007, Report on Sky Quality Meter, Version L. Tech. Rep. ISTIL. Available at: http://unihedron.com/projects/sqm-l/sqmreport2.pdf

Danish Energy Agency CLASP European Programme Energy Piano, 2015, European LED Market Evolution and Policy Impacts. European Commission Available at: http://clasp.ngo/~/media/Files/SLDocuments/2015/DEA%20-%20CLASP%20Report%20on%20European%20LED%20Market_final.ashx

den Outer P., Lolkema D., Haaima M., Hoff R. v. d., Spoelstra H., Schmidt W., 2011, Sensors, 11, 9603

den Outer P., Lolkema D., Haaima M., van der Hoff R., Spoelstra H., Schmidt W., 2015, Sensors, 15, 9466

Eloholma M., Halonen L., 2006, Leukos, 2, 263

Esposito F., Pavese G., Serio C., 2001, Atmos. Environ., 35, 5093

Falchi F., 2011, MNRAS, 412, 33

Falchi F. et al., 2016, Sci. Adv., 2, e1600377

Fröhlich C., Shaw G. E., 1980, Appl. Opt., 19, 1773

Fukugita M., Shimasaku K., Ichikawa T., 1995, PASP, 107, 945

Johnson H., Morgan W., 1953, ApJ, 117, 313

Judd D. B., 1951, Proc. Twelfth Session CIE Stockholm, 1, 11

Katona T. M., Pattison P. M., Paolini S., 2016, Ann. Rev. Chem. Biomol. Eng., 7, 263

King I., 1952, ApJ, 115, 580

Kolláth Z., Dömény A., Kolláth K., Nagy B., 2016, J. Quant. Spectrosc. Radiat. Transfer, 181, 46

Kyba C. C., 2013, Loss of the Night Citizen Science Project. Available at: http://lossofthenight.blogspot.com.es/2013/08/first-blog-post-welcome-to-official.html

Kyba C., Ruhtz T., Fischer J., Hölker F., 2012, MNRAS, 425, 701

Kyba C. C. et al., 2013, Sci. Rep., 3, 1835

Kyba C. C. et al., 2015, Sci. Rep., 5, 8409

Oke J., Gunn J., 1983, ApJ, 266, 713

Pun C. S. J., So C. W., 2012, Environ. Monit. Assess., 184, 2537

Pun C. S. J., So C. W., Leung W. Y., Wong C. F., 2014, J. Quant. Spectrosc. Radiat. Transfer, 139, 90

Puschnig J., Posch T., Uttenthaler S., 2014, J. Quant. Spectrosc. Radiat. Transfer, 139, 64

Rea M. S., Bullough J. D., Freyssinier-Nova J. P., Bierman A., 2004, Light. Res. Technol., 36, 85

Rendtel J., Arlt R., McBeath A., 1995, Handbook for Visual Meteor Observers. IMO Monograph No. 2. Intentional Meteor Organization, Potsdam

Riegel K. W., 1973, Science, 179, 1285

Sánchez de Miguel A., 2015a, PhD thesis, Universidad Complutense de Madrid

Sanchez de Miguel A., 2015b, First Use of ISS Astronaut Pictures for Light Pollution Studies – IAU. Available at: https://www.iau.org/news/pressreleases/detail/iau1510/

Smith T., Guild J., 1931, Trans. Opt. Soc., 33, 73

Spoelstra H., 2014, J. Quant. Spectrosc. Radiat. Transfer, 139, 82

Tapia Ayuga C., Sánchez de Miguel A., Zamorano Calvo J., 2015, LICA-UCM Lamps Spectral Database. LICA Reports. Madrid

Williams D. R., 2010, Moon Fact Sheet. NASA Goddard Space Flight Center, Greenbelt, MD. Available at: http://nssdc.gsfc.nasa.gov/planetary/factsheet/moonfact.html

Zamorano J., Sánchez de Miguel A., Alfaro E., Martınez-Delgado D., Ocana F., Nievas M., Gómez Castano J., 2013, in Guirado J. C., Lara L. M., Quilis V., Gorgas J., eds, Highlights of Spanish Astrophysics VII, Proceedings of the X Scientific Meeting of the Spanish Astronomical Society. SEA, Barcelona, p. 962

Zamorano J., Nievas M., Sánchez de Miguel A., Tapia C., García C., Pascual S., Ocaña F., Gallego J., 2015, IAU General Assembly, 22, 54626

Zamorano J. et al., 2016, J. Quant. Spectrosc. Radiat. Transfer, 181, 52

SUPPORTING INFORMATION

Supplementary data are available at *MNRAS* online.

colores_espectros_SQM_SC_BGj_6k.png

colores_espectros_SQM_SC_BGj_60k.png
colores_espectros_SQM_SC_BGj_30k.png
colores_espectros_SQM_SC_BGj_15k.png
colores_espectros_SQM_SC_BGj_100k.png
colores_espectros_SQM_BVj6k.png
colores_espectros_SQM_BVj30k.png
colores_espectros_SQM_BVj15k.png
colores_espectros_SQM_BVj100k.png

Please note: Oxford University Press is not responsible for the content or functionality of any supporting materials supplied by the authors. Any queries (other than missing material) should be directed to the corresponding author for the article.

This paper has been typeset from a TEX/LATEX file prepared by the author.